Articulated legs allow energy optimization across different speeds for legged robots with elastically suspended loads

Anna Astolfi, *Member, IEEE,* and Marcello Calisti *Member, IEEE*

***Abstract*— Legged robots are a promising technology whose use is limited by their high energy consumption. Biological and biomechanical studies have shown that the vibration generated by elastically suspended masses provides an energy advantage over rigidly carrying the same load. The robotic validation of these findings has only scarcely been explored in the dynamic walking case. In this context, a relationship has emerged between the design parameters and the actuation that generates the optimal gait. Although very relevant, these studies lack a generalizable analysis of different locomotion modes and a possible strategy to obtain optimal locomotion at different speeds. To this end, we propose the use of articulated legs in an extended Spring-Loaded Inverted Pendulum (SLIP) model with an elastically suspended mass. Thanks to this model, we show how stiffness and damping can be modulated through articulated legs by selecting the knee angle at touch-down. Therefore, by choosing different body postures, it is possible to vary the control parameters and reach different energetically optimal speeds. At the same time, this modeling allows the study of the stability of the defined system. The results show how suitable control choices reduce energy expenditure by 16% at the limit cycle at a chosen speed. The demonstrated strategy could be used in the design and control of legged robots where energy consumption would be dynamically optimal and usage time would be significantly increased.**

I. Introduction

Legged robots are a rising technology for moving over rough terrain. They show a dexterity far superior to wheeled or tracked vehicles, especially on natural terrains with discontinuities, asperities, or obstructions [1]. Despite their promising performances, their usage in real-world scenarios is still limited by several challenges, including their short operational time [2], [3]. To tackle this problem, energy efficiency has to be optimized. In this regard, embedding compliance into the leg's structure has proved beneficial as springs contribute to impact absorption and energy return [4]. Moreover, springy legs also help to stabilize the motion [5], therefore becoming of paramount importance in dynamically stable locomotion [6], [7], [8].

Beside leg compliance, biological and biomechanical studies showed that wobbling masses, such as soft tissues and visceral mass, contribute to power absorption and return [9], [10]. Particularly, the visceral mass, which is elastically suspended in the abdominal cavity, moves harmonically during walking and running, providing an energetic advantage [11] with respect to rigidly carrying the same load [12], [13]. Although these evidences have been employed for the smart design of carriage systems (e.g., backpack [14]), it is not yet common to design legged robots with a load suspension system to carry electronics, batteries, and more.

To date, only a few studies dealt with the subject. In [15], the effects of an additional mass-spring-damper mechanism on the self-stabilizing properties of a SLIP model have been investigated. The authors reported an increase in self-stability and robustness to perturbation with respect to the SLIP model, but they did not investigate the effect of the suspended load on energy efficiency. They used a step-to-fall analysis [16] to assess stability and perturbations in the landing velocity to quantify robustness. They fixed most of model parameters to values compliant with the human body. In [17], [18], two masses oscillating in the vertical direction (as in dynamic walking gait) were used to investigate the energy saving based on the selection of the suspended load stiffness, damping, and leg actuation frequency. This investigation was used as design criteria for selecting the legs and the suspended load on a RHex robot [19] performing a dynamic walking gait. The results reported a significant decrease in energy consumption up to 24% compared with a rigidly attached load.

Although the results were promising, this conceptual idea is limited to a specific design (stiffness, damping) and actuation frequency, therefore to a specific forward speed, impairing the versatile use of this approach. However, in articulated legs (i.e. legs with a knee joint) stiffness and damping could be modulated by selecting a specific knee-angle at touchdown [20], with advantages in terms of stability and controllability [21], [22]. By building upon the idea of elastically suspended load on springy legs, we hypothesize that articulated legs could be exploited to optimize energy efficiency. In fact, by controlling the angle of attack and the knee angle at touchdown, it is possible to obtain optimal locomotion at different speeds without mechanically changing the body of the robot.

Therefore, in this work we propose a practical design strategy to exploit the energetic advantage of the elastically suspended load when moving at a selected speed. We demonstrate the concept by extending the simplest running model, i.e., the Spring-Loaded Inverted Pendulum (SLIP) [23], [16], [24], to include leg actuation and damping in an articulated leg as well as an elastically suspended load. The model is presented in dimensionless terms to simplify the translation of results for different design choices and gaits. To our knowledge, this is the first work showing the effect

*This work was not supported by any organization

A. Astolfi, and M. Calisti are with the Biorobotics Institute, Scuola Superiore Sant'Anna and Department of Excellence in Robotics and Artificial Intelligence, Pontedera(PI), Italy, e-mail: (a.astolfi@santannapisa.it, mcalisti@lincoln.ac.uk).

M. Calisti is currently with the Lincoln Institute for Agri-food Technologies, Lincoln, UK.

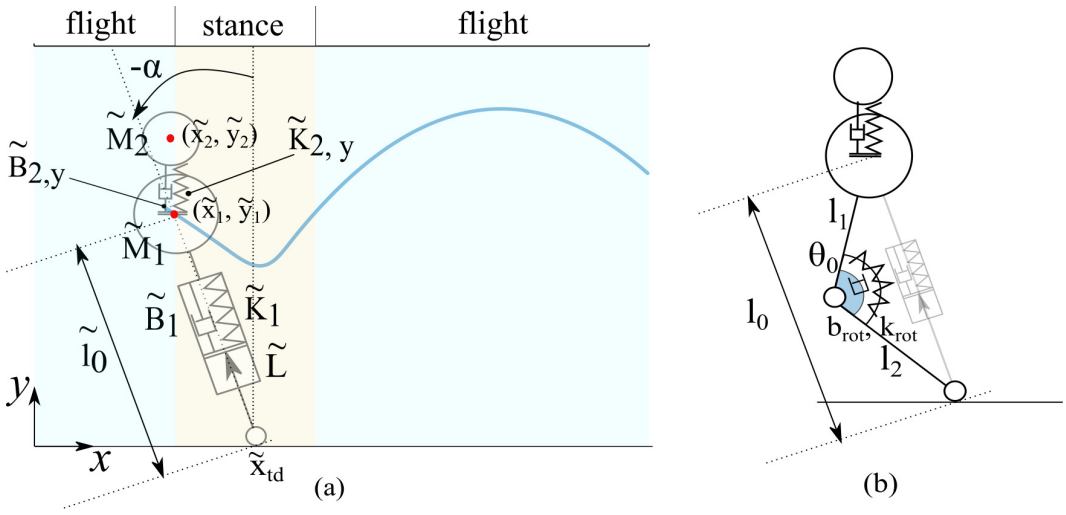

Fig. 1. (a) A modified SLIP model which include a suspended load, leg actuation and damping. Position variables, control and design parameters are shown. (b) Equivalent model with the articulated leg's additional degree of freedom θ_0.

of suspended loads in a running model.

II. Materials and Methods

A. Coupled Spring Mass Damping Model with flight Phases

The Equations of Motion for a SLIP model enriched with damping, actuation, and a load suspension system are presented in this section, and supported by Fig.1. With reference to Fig.1a, during dynamic gaits the system undergoes phases of ground contact and flight phases. These can be described by four differential equations each, the main difference between the two sets is a term of elastic interaction with the ground, featured in the stance phase and lacking in the flight phase. The system state is defined by the horizontal and vertical positions of the main mass M_1, the horizontal and vertical positions of the suspended load mass M_2 and their velocities. To get untied from a specific parameterization and make the description as generic as possible, the equations are presented in dimensionless form by normalizing the length quantities to the resting leg length l_0 and the time to $t_c = \sqrt{l_0/g}$.

The stance phase begins when the foot touches the ground in position x_{td}. We impose the leg to be at its rest length l_0, tilted of an angle α from the vertical axis (angle of attack), right before the touch-down event (TD). Therefore the TD is geometrically defined by:

$$y_1 = cos(\alpha) \tag{1}$$

Afterwards, the leg compress and re-extend, according on the evolution of the state variables, under the effects of both active and passive forces. Specifically the state variables are ruled by the following equations of motion:

$$\begin{aligned} \ddot{x}_1 = \; & B_{2,x}(\dot{x}_2 - \dot{x}_1) + K_{2,x}(x_2 - x_1) + \\ & B_1(\dot{L}_x - \dot{x}_1) + K_1(1 - l + L)\frac{x_1 - x_{td}}{l} \end{aligned} \tag{2}$$

$$\begin{aligned} \ddot{y}_1 = \; & B_{2,y}(\dot{y}_2 - \dot{y}_1) + K_{2,y}(y_2 - y_1) + \\ & B_1(\dot{L}_y - \dot{y}_1) + K_1(1 - l + L)\frac{y_1}{l} - 1 \end{aligned} \tag{3}$$

$$\ddot{x}_2 = -\frac{B_{2,x}}{M_{1,2}}(\dot{x}_2 - \dot{x}_1) - \frac{K_{2,y}}{M_{1,2}}(x_2 - x_1) \tag{4}$$

$$\ddot{y}_2 = -\frac{B_{2,y}}{M_{1,2}}(\dot{y}_2 - \dot{y}_1) - \frac{K_{2,y}}{M_{1,2}}(y_2 - y_1) - 1 \tag{5}$$

The resulting system is fully described by five dimensionless groups, which represent the leg stiffness and damping K_1 and B_1, the suspension system stiffness and damping K_2 and B_2, and the ratio between the suspended mass and the main body mass $M_{1,2}$. The dimensionalization is described in Tab.I, where the corresponding dimensional variables are represented with a tilde (Fig.1(a)).

Unlike the classical SLIP model, which is energy conservative and therefore does not include any active force term, our model also includes leg actuation, realized by means of a serial elastic actuator (SEA), with actuation law $L(t)$. The actuation function L can be any function of time. In this case, we employed a sinusoidal law, represented by the dimensionless parameters A and ω, as already proposed in [17]. According to this function, the amount of energy that can be injected into the system through the SEA is restricted.

$$L = Asin(\omega(t - t_{td})) \tag{6}$$

The lift-off (LO) condition occurs when the elastic element gets unloaded:

$$l(t) = 1 + L(t) \tag{7}$$

resulting in the disappearance of the relative terms during the flight phase, which is equivalent to set $K_1 = 0$ and $B_1 = 0$ in Eq.(2)-(3). At each LO event, the leg length is immediately restored to l_0, ready for the next TD.

Again, with respect to the SLIP model our model requires two extra equations (Eq.(3)-(4)) and two extra force terms, to describe the dynamics of the suspended mass and the interaction forces between the two masses, respectively. The

interaction forces are the same for both masses, but with opposite directions, and the resulting acceleration is scaled by the ratio between the two masses.

TABLE I
DIMENSIONLESS PARAMETERS AND VARIABLES

$l_0[m]$	Resting leg length
$g[m/s^2]$	Gravity acceleration
$t_c = \sqrt{l_0/g}[s]$	scaling factor
$x_1 = \tilde{x}_1/l_0$	M1 Horizontal position
$x_2 = \tilde{x}_2/l_0$	M2 Horizontal position
$y_1 = \tilde{y}_1/l_0$	M1 Vertical position
$y_2 = \tilde{y}_2/l_0$	M2 Vertical position
$A = \tilde{A}/l_0$	Oscillation Amplitude
$\omega = \tilde{\omega}t_c$	Oscillation frequency
α	angle of attack
θ_0	initial inter-segment angle
$B_1 = (\tilde{B_1}/\tilde{M_1})t_c$	Leg damping
$K_1 = (\tilde{K_1}/\tilde{M_1})t_c^2$	Leg stiffness
$B_{2,y} = (\tilde{B_{2,y}}/\tilde{M_1})t_c$	Suspended Load damping
$K_{2,y} = (\tilde{K}_{2,y}/\tilde{M_1})t_c^2$	Suspended Load stiffness
$M_{1,2} = \tilde{M_2}/\tilde{M_1}$	Load-Body weight ratio

TABLE II
RANGES OF PARAMETERS
AND INITIAL CONDITIONS TESTED

Control Parameters			
	$\tilde{A}$	6e-2 m	
	$\tilde{\omega}$	21 rad/s	
Design Parameters			
B_1	[0-0.2],[0.6-17]	$B_{2,y}$	[0.011-0.572]
K_1	[0-82], [400-500]	$K_{2,y}$	[1.25-6.26]
$M_{1,2}$	[0.14-0.51]		
Initial Conditions			
$\dot{x}_{2,}0$	[-5.5 5.5]	$\dot{x}_{2,0}$	$\equiv \dot{x}_{1,0}$
$y_1, 0$	$[cos(\alpha), 1.05/l_0]$	$y_{2,0}$	$\equiv y_{1,0}$
$\dot{y}_{1,0}$	0	$\dot{y}_{2,0}$	0

It is worth mentioning that this system is similar to a double pendulum, and therefore it might exhibit chaotic behavior. Under the assumption that we can constrain the oscillations of the suspended load only to the vertical direction y, we can avoid chaotic behaviors by imposing high stiffness and damping values in the x direction. In our specific simulations, we imposed $K_{2,x} = 10K_1$ e $B_{2,x} = 10B_1$, as in [18]. We consider this assumption acceptable based on feasible implementations, i.e. with leaf springs, and with controllers that minimize the pitching angle of the main body [25], [17].

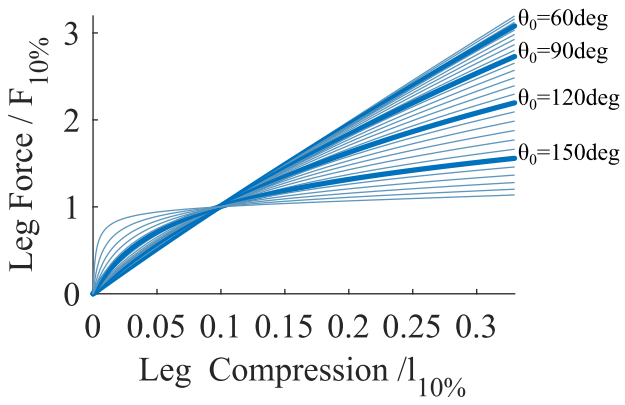

Fig. 2. Leg Force against Leg compression for different knee-angles at TD. Axis are normalized at 10% of leg compression ($l_{10\%}$) and the corresponding force ($F_{10\%}$), to better show the behavior for small deformations.

B. Leg Articulation

We hypothesized that the use of an articulated leg, which offers a modulation of the stiffness along the direction of elongation, will allow to select an energetically optimal gait at each locomotion speed.
According to Fig.1b, we can consider an articulated leg, made by two segments l_1 and l_2, and a torsional spring of constant stiffness k_{rot} at the joint between the two. Then the stiffness k of an equivalent non-segmented leg is a function of the angle between the two segments θ_0 at the TD event according to:

$$k = k_{rot}\frac{(\theta - \theta_0)l}{l_1 l_2 sin(\theta)(l - l_0)} \tag{8}$$

with l and l_0 related to θ and θ_0 by the cosine rule. We aim to directly extend the results and the model of [17] by adopting Eq. (2)-(5) and to include an articulated leg by using the leg stiffness obtained as linearization of k_{rot} under the selection of θ_0 according to Eq. (8). In Fig.2, we show the leg force against the leg compression, for different values of θ_0, the x-axis is normalized at 10% of leg compression and the y-axis for corresponding leg force. The linearization of Eq. (8) holds only in a working interval of θ_0 and for small deformations of knee-angle. We will focus on these for the analysis, but we will report also results out of this range for completeness of description.

C. Parameter Selection and Model Analysis

The dynamic system in Eq. (2)-(5) features 6 periodic state variables $\mathbf{q} = [\dot{x}_1, \ y_1, \ \dot{y}_1, \ \dot{x}_2, \ y_2, \ \dot{y}_2]$, 5 design parameters $\mathcal{D} = [B_1, B_2, K_1, K_2, M_{1,2}]$, and 3 control variables $\mathcal{C} = [A, \omega, \alpha]$. Each set $\mathcal{S} = [\mathcal{D}, \mathcal{C}]$ completely describe a dynamical system, whose fixed points (FPs) and their stability can be investigated.
Therefore, we firstly spanned different combinations of $\mathcal{S}$ to broadly describe the system, and to find limit cycles, i.e. stable periodic orbits, corresponding to different stable locomotion modalities. Subsequently, we focused only on combinations of $\mathcal{S}$ that were consistent with human parameters. With respect to these we analyzed the influence of α and

θ_0 on the average positive power (APP) with the objective of confirming our hypothesis. The APP is computed from the leg force and the actuator speed as in [17]:

$$\begin{aligned} F &= K_1(\Delta l(t) - L(t)) + B_1(\dot{\Delta l}(t) - \dot{L}(t)) \\ V &= \dot{L}(t) \\ P &= FV \\ APP &= \frac{\int P(P \geq 0)^2 dt}{T} \end{aligned} \tag{9}$$

Concerning the first objective, i.e. providing a comprehensive overview of the model, we started by feeding the system of Eq. (2)-(5), completely defined by a set $\mathcal{S}$, with 100 initial conditions. For each of these, we searched FPs as intersections of $\mathbf{q}$ with a Poincarè section orthogonal to $\dot{y}_1$, and passing by the apex state $\dot{y}_1 = 0$. FPs are found numerically as zeros of the function $g(\mathbf{q}) = f(\mathbf{q}) - \mathbf{q}$, with $f(\mathbf{q})$ the *stride function* of $\mathbf{q}$, using the Newton-Raphson algorithm (as in [26]), with an error of $|g(\mathbf{q}^*)| \leq$ 1e-6. Stability was assessed from the maximum Floquet multipliers, i.e. the absolute value of the maximum eigenvalue ($|\lambda_{max}|$) of the Jacobian of $f(\mathbf{q}^*)$ for a number of perturbations of $\mathbf{q}^*$. When a limit cycle is found for a given $\mathcal{S}_i$ it was used as initial condition for the search in $\mathcal{S}_i + \delta\mathcal{S}$ to fasten the search.
The ranges of parameters and initial conditions used for $\mathcal{S}$ are reported in Tab.II.
Throughout the analysis, we fixed the dimensional control variables $\tilde{A}$ and $\tilde{\omega}$ according to reasonable values for the visceral mass oscillations and time duration of the stance phase [12], [13]. The angle of attack α was varied according to the leg stiffness $\tilde{K}_1$ as expected from SLIP model [16], according to:

$$K_1 = \frac{const}{1 - sin(\alpha)} \tag{10}$$

with $const = 1700$.
In Section III-A we show model outcomes under variations of $\mathcal{D}$. The second contribution, whose results are described in Sections III-B, shows the energy advantage of a suspended load and an articulated leg during running dynamics. As this analysis is related to the control aspect of locomotion rather than on the design, we set the design parameters of the main body to human compliant values. Particularly, the dimensional stiffness $\tilde{K}_1$ in the range $19 - 50 \cdot 10^4 N/m$, the leg length $l_1 + l_2 \in [0.9 - 1.05]$ m, as in [16], the total body mass $\tilde{M}_1 + \tilde{M}_2 \simeq 70kg$ with $M_{1,2} = 0.14$, according to [27], [12]. Without loss of generality, we assumed $l_1 = l_2$.

III. Results and Discussions

A. Model analysis under variations of design parameters

The model we introduced with Eq.(2)-(5) allows to analyze how dimensionless parameters affect the locomotion, and also to investigate a gait variability which was not reported by the previous model [17], [15]. In particular, we found different limit cycles which correspond to qualitatively different gaits, namely running [16], punting [28], and hopping.

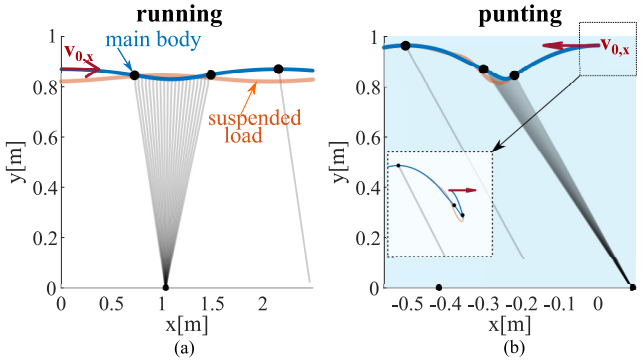

Fig. 3. (a) A typical running trajectory in the x-y plane. In blue the main body trajectory, in orange the suspended load oscillation. (b) A typical punting trajectory. The initial velocity can be either positive or negative (within the basin of attraction) as only the angle of attack defines locomotion direction.

As shown in Fig.3(a), the running dynamics features a significant leg swing about the touchdown point x_{td}, i.e. the angle of attack changes from negative to positive values. Instead, the punting gait, Fig.3(b), is characterized by a small swinging of the leg about x_{td}, with the angle of attack not changing sign. Hopping is characterized by the same leg behavior, with the significant difference that the body experiences longer flight phases and higher vertical excursions. As another difference between hopping and punting, in the former, the initial velocity dictates the direction of locomotion, which depends only on the angle of attack in punting, as shown in the highlight panel of Fig.3(b).

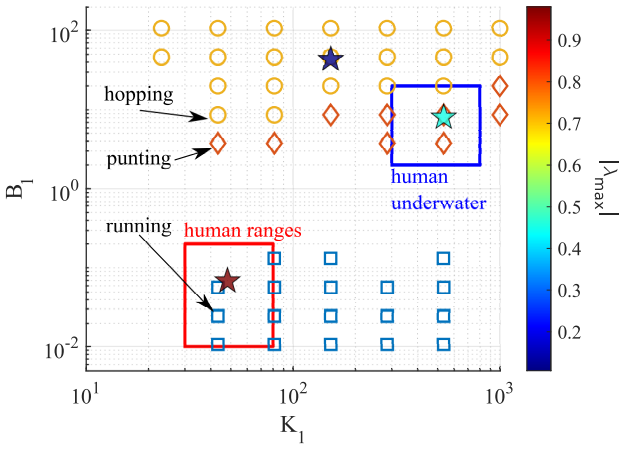

Fig. 4. Different gaits discovered when the leg parameters K_1, B_1 were changed. showing qualitatively different gaits for different ranges of leg parameters.

Fig.4 gives an overview of the gait discovered in the different region of the $B_1 - K_1$ plane. Different color areas represents sets among which major qualitative differences allow the classification into the three different gaits previously described (see also the Multimedia Materials). In all the conditions showed, the value of the suspended load stiffness K_2 is varied so that the ratio with respect to K_1 is held constant to 0.2. We highlighted, with red and blue squares, the regions that represents human proportions

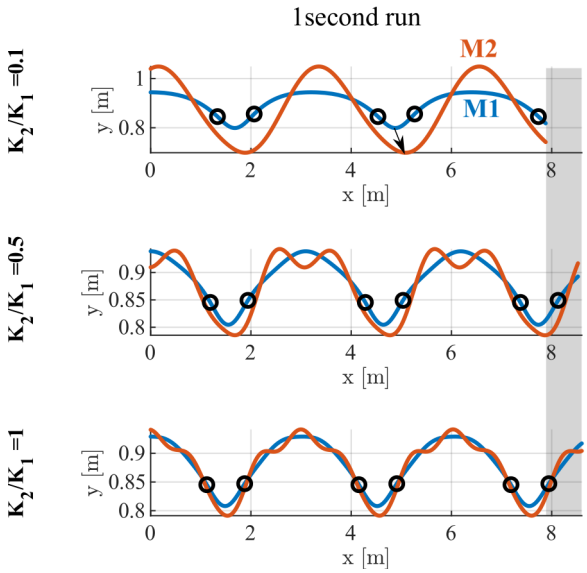

Fig. 5. The suspended load stiffness influences on performances is marginal. The velocity is almost unvaried. The influence on power saving can be due to the higher out-of-phase motion between the main body mass (in blue) and the suspended load mass (orange).

between parameters in $\mathcal{D}$ and control parameters in $\mathcal{C}$, when moving on land (red) and underwater (blue). The range of $K_1 \in [30-80]$ and $B_1 \in [0-0.2]$ revealed the presence of a "running" dynamics. In fact the stiffnes values are in line with those of pure SLIP in [16], while a small damping is required to compensate the energy injected through actuation. In the region $K_1 \geq 400$ and $B_1 \in [0.5-16]$ we found the "punting" dynamics, typical of the underwater locomotion, whereas for further higher values of B_1 the punting evolves into the "hopping" dynamics.

These findings are coherent with the emergence of punting instead of running in the underwater scenario. Due to the buoyancy force, the apparent gravity perceived by an immersed body is reduced. The consequences of this is that if the same body moves underwater the adimensional stiffness K_1 will be increased as a result of $\tilde{K}_1 l_0 >> \tilde{M}_1 g$. The emergence of punting over running for increasing values of damping has been reported also by previous studies on locomotion in resistive environments [29]. In their analysis, the authors hypothesized that despite less efficient in term of locomotion speed, the punting could emerge spontaneously as a result of increasing damping forces from the environment in completely submerged legs. Here we complement their results with ours, which highlight how an increasing leg damping can also guide such a gait transition.

Concerning stability, we observed that it increases when both K_1 and B_1 increase. In fact, for the three conditions marked with stars in Fig.4, the system's $|\lambda_{max}|$ moves from 0.979 in the running dynamics (lowest B_1) to 0.910 during punting, down to 0.158 in the hopping (highest B_1). This agrees with previous results on single mass systems where local stability is improved by damping [28].

Furthermore, in accordance with previous works [17], we found that the suspended mass negatively affects the locomotion stability, especially for the low values investigated (K_2 =$0.2K_1$ in our analysis), even though we were still able to find converging behaviors ($|\lambda_{max}| < 1$). On the other hand, we ignored higher values of the suspended load stiffness ($K_2 >= 0.7K_1$), as they have shown to negatively affect the power saving [17].

Moreover, we showed that the suspended load parameters do not affect the type of gait, that is determined mainly by leg parameters, and also their influence on the performances (e.g., forward velocity) is almost irrelevant. As an example, in Fig.5 we report the effect of variations of K_2 on velocity. By increasing K_2 from 10% to 100% of the leg stiffness the induced velocity variation is just 0.35 m/s over an average speed of 8.25 m/s. On the other hand it has a significant effect on power saving allowing to reduce up to 10% the energy requirements in the three examples shown.
This can be explained by the variation of the out-of-phase oscillation of the suspended mass [17], which is maximized at lower K_2 values, and it is for the first time associated also with the speed of locomotion. In fact, if we want a legged robot to be always energetically optimal, it is required that the power consumption can be defined by a controllable variable, without affecting the forward velocity. The design parameters of the suspension system should be thought as a pure design choice and they should not be varied during the locomotion, as their effect on performances has been showed here to be marginal with respect to leg parameters.

B. Energy saving promoted by suspended loads can be modulated by leg articulation

Once we found parameter ranges allowing a stable running gait, we investigated the dependence of performances and power requirements for an articulated leg with respect to control variables α and θ_0. For our in-depth investigation, we used sets $\mathcal{S}$ coherent with human parameters, without lack of generality to extend the results to other animals or robots.

In Fig.6(a) we show the isovelocity lines over-imposed to the APP curve. For the tested set, we did not find a global minimum as both the energy and velocity have monotonic trends. Particularly, the APP decreases when the knee angle θ_0, and according to Eq.(8) the stiffness, increases. The effect of α in the variation of APP seems marginal. On the other hand, the speed is mainly influenced by α, in the tested ranges, and only slightly by θ_0.

The result seems to suggest that higher postures, i.e. high values of θ_0, are preferred from the energetic point of view, and therefore that a leg design that only offers modulation of α would be disadvantageous in the context of energy optimization. This confirms our initial hypothesis that articulated legs could be used to optimize energy consumption at different speeds. As highlighted in Fig.6(a), once a specific speed is selected by α, θ_0 can be increased up to a certain level which minimizes energy consumption. As can be observed in Fig. 6(d), higher postures, featuring higher stiffnesses, result in gaits with smaller duty factors

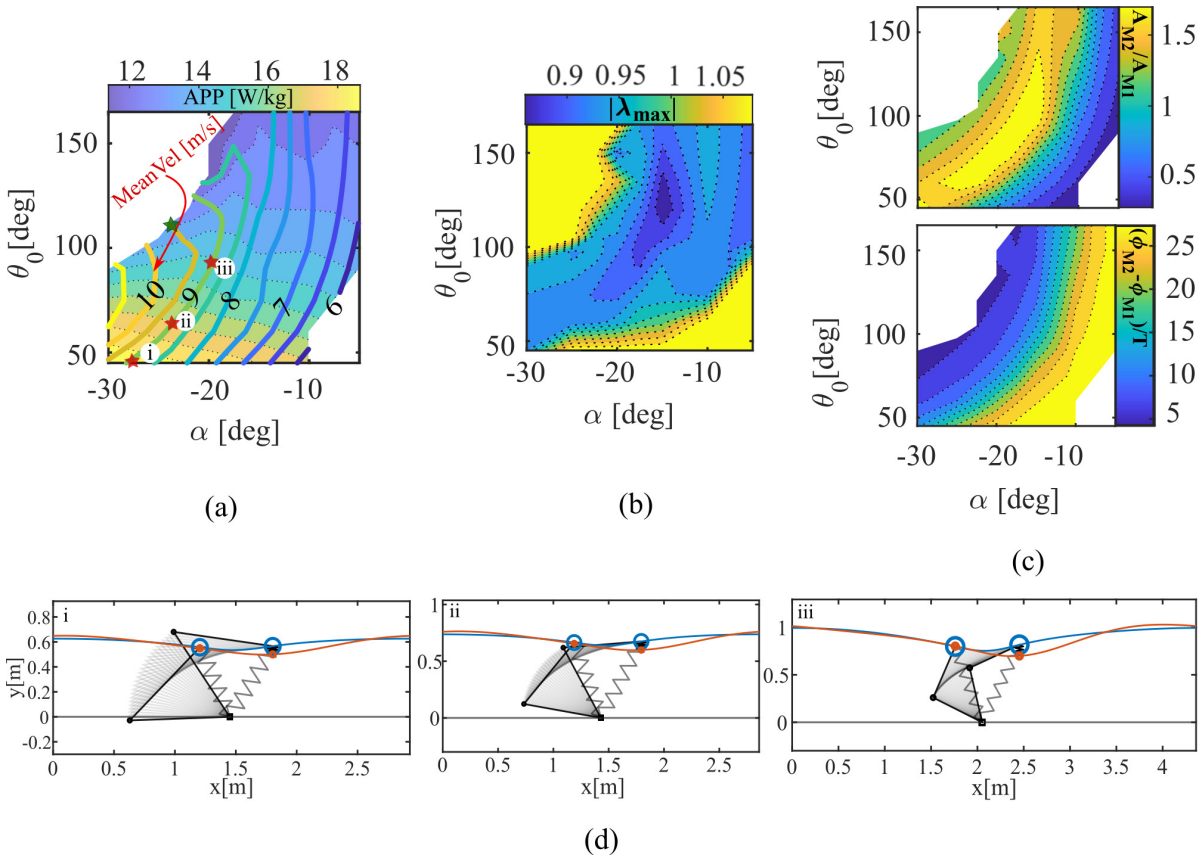

Fig. 6. (a) APP and iso-velocity lines in the α-θ_0 plane. (b) Corresponding maximum Floquet multiplier for each gait in (a). (c) Amplitude ratio between suspended mass and main mass and Phase Difference between the trajectory of the two masses, as a function of control parameters α and θ_0. (d) Isovelocity solutions for moving at 9m/s with different control parameters. The energy efficiency improves moving from left to right.

(ratio between stance period and whole gait period).

It has to be noted that by increasing θ_0 we are correspondingly slightly decreasing the stability of the system, Fig.6(b), and that maximum stability has been found in the neighborhood of $\alpha = -15deg$ and $\theta_0 = 125deg$. Very high postures and more horizontal angle of attack, as well as very low postures and vertical angle of attack, result in unstable gaits. It appears that energy saving can be optimized at the expense of the stability of the system. This might be related to the dynamic of the suspended load with respect to the main body.

In Fig.6(c), we reported the oscillation amplitude of the suspended mass relative to the main body mass and the phase shift between the two normalized over the gait period. Our results show that the velocity (and therefore the angle of attack) defines the phase shift between the two masses. At the same time, a wider amplitude of oscillations seems to be related to more stable gaits. This result is partially in contrast with literature results [17], which sustained that the energy efficiency was due to a 180 deg phase-shift between the two masses. We attribute this discrepancy to the presence of long flight phases in our model, that were completely ignored in previous investigations on dynamic walking locomotion. In fact, flight phases do not play a role in power management as they are purely passive except for forces between the two masses under the effect of the spring and damper of the suspension system. Therefore even a slight phase shift occurring within the stance phase can be beneficial for energy saving, as well as the reduction of the duty factor.

The initial condition spanned throughout the analysis may also play a role in the emerging trends, as we only investigated the evolution of the system from initial conditions where the suspended mass and the main body mass were moving in the same way, (initial velocity in x is the same and in y is at rest). Due to the complexity of the system under analysis, we did not extract a general rule for these behaviors. Previous works [17], showed an energy optimum as a function of K_2 and M_2 when fixing the actuation. The interdependence of these variables can explain the lack of minimum in our investigation: as we vary K_1, under the variation of θ_0, we also modify the ratio K_2/K_1 in a way that can be sub-optimal, if we consider all the control parameters that have an effect on speed and power. Of course, this analysis can be complemented with additional investigations, for instance on the actuation strategy, to further optimize the power consumption and its saving.

Eventually, we computed the APP saving with respect to rigidly carrying the load. The maximum saving is 22% for the configurations $\alpha = -20deg$ and $\theta_0 = 135deg$, while it reaches 16% at $\alpha = -24deg$ and $\theta_0 = 113deg$ (reported

as a green star in Fig. 6(a)). It is worth mentioning that the latter value falls within ranges of θ_0 where the linearization introduced in Eq. 8 (see Fig.2) is acceptable, and therefore our results found direct application. On the other hand, for the former value, comparable energy savings can be achieved by employing a different actuation strategy. Future directions of this investigation require the translation to a robotic system to verify the demonstrated trends in energy saving. Despite the increased complexity of a robotic implementation with respect to the mathematical description addressed in this work, we are confident that simple controllers employing the same control law of the model and acting within the stability regions of the modeled dynamics will prove the results, at least qualitatively, as already demonstrated in previous works [21], [30], [19].

IV. CONCLUSIONS

In this paper, we showed how articulated legged robots could benefit from a suspended load design. By significantly extending the existing model and by performing in-depth computational analysis, we confirmed that, in a suspended load configuration, small values of K_2 promote energy efficiency while higher values of B_2 improve stability. Both parameters are part of the design specifications, that cannot be altered easily after fabrication.

In contrast, leg control parameters play a significant role: their choice allows to decrease energy consumption, up to 16%, without affecting the speed neither requiring mechanical modification of the system. The stiffness modulation offered by an articulated leg design allows the selection of the optimal stance (i.e. θ_0) for a desired speed. Our linearization holds in the range $45 \leq \theta_0 \leq 120$ deg and can be directly employed in articulated legged systems, while for $\theta_0 \rightarrow 180$ deg the non linear behaviour would require a different elongation law.

The proposed approach can be used to design versatile articulated legged robots, which operational time would be increased by selecting the optimal actuation strategy dynamically.

REFERENCES

[1] C. D. Bellicoso, M. Bjelonic, L. Wellhausen, K. Holtmann, F. Günther, M. Tranzatto, P. Fankhauser, and M. Hutter, "Advances in real-world applications for legged robots," *Journal of Field Robotics*, vol. 35, no. 8, pp. 1311–1326, 2018.

[2] Z. Fu, A. Kumar, J. Malik, and D. Pathak, "Minimizing energy consumption leads to the emergence of gaits in legged robots," *arXiv preprint arXiv:2111.01674*, 2021.

[3] S. Kim and P. M. Wensing, "Design of dynamic legged robots," *Foundations and Trends in Robotics*, vol. 5, no. 2, pp. 117–190, 2017.

[4] M. Hutter, C. D. Remy, M. A. Höpflinger, and R. Siegwart, "Slip running with an articulated robotic leg," in *2010 IEEE/RSJ International Conference on Intelligent Robots and Systems*. IEEE, 2010, pp. 4934–4939.

[5] M. Calisti, G. Picardi, and C. Laschi, "Fundamentals of soft robot locomotion," *Journal of The Royal Society Interface*, vol. 14, no. 130, p. 20170101, 2017.

[6] J. Reher, W.-L. Ma, and A. D. Ames, "Dynamic walking with compliance on a cassie bipedal robot," in *2019 18th European Control Conference (ECC)*. IEEE, 2019, pp. 2589–2595.

[7] G. Urbain, V. Barasuol, C. Semini, J. Dambre *et al.*, "Effect of compliance on morphological control of dynamic locomotion with hyq," *Autonomous Robots*, vol. 45, no. 3, pp. 421–434, 2021.

[8] R. Altendorfer, U. Saranli, H. Komsuoglu, D. Koditschek, H. B. Brown, M. Buehler, N. Moore, D. McMordie, and R. Full, "Evidence for spring loaded inverted pendulum running in a hexapod robot," in *Experimental Robotics VII*. Springer, 2001, pp. 291–302.

[9] T. Kamimura, K. Sato, D. Murayama, N. Kawase, and A. Sano, "Dynamical effect of elastically supported wobbling mass on biped running," in *2021 IEEE/RSJ International Conference on Intelligent Robots and Systems (IROS)*. IEEE, pp. 4071–4078.

[10] R. C. Riddick and A. D. Kuo, "Soft tissues store and return mechanical energy in human running," *Journal of Biomechanics*, vol. 49, no. 3, pp. 436–441, 2016.

[11] L. C. Rome, L. Flynn, and T. D. Yoo, "Rubber bands reduce the cost of carrying loads," *Nature*, vol. 444, no. 7122, pp. 1023–1024, 2006.

[12] A. E. Minetti and G. Belli, "A model for the estimation of visceral mass displacement in periodic movements," *Journal of biomechanics*, vol. 27, no. 1, pp. 97–101, 1994.

[13] R. M. Alexander, "On the synchronization of breathing with running in wallabies (macropus spp.) and horses (equus caballus)," *Journal of Zoology*, vol. 218, no. 1, pp. 69–85, 1989.

[14] J. Ackerman and J. Seipel, "A model of human walking energetics with an elastically-suspended load," *Journal of biomechanics*, vol. 47, no. 8, pp. 1922–1927, 2014.

[15] S. E. Masters and J. H. Challis, "Increasing the stability of the spring loaded inverted pendulum model of running with a wobbling mass," *Journal of Biomechanics*, vol. 123, p. 110527, 2021.

[16] A. Seyfarth, H. Geyer, M. Günther, and R. Blickhan, "A movement criterion for running," *Journal of Biomechanics*, vol. 35, no. 5, pp. 649–655, 2002.

[17] J. Ackerman and J. Seipel, "Energy efficiency of legged robot locomotion with elastically suspended loads," *IEEE Transactions on Robotics*, vol. 29, no. 2, pp. 321–330, 2013.

[18] ——, "Coupled-oscillator model of locomotion stability with elastically-suspended loads," *Proceedings of the ASME Design Engineering Technical Conference*, vol. 1, no. PARTS A AND B, pp. 199–205, 2011.

[19] U. Saranli, M. Buehler, and D. E. Koditschek, "Rhex: A simple and highly mobile hexapod robot," *The International Journal of Robotics Research*, vol. 20, no. 7, pp. 616–631, 2001.

[20] J. Rummel and A. Seyfarth, "Stable running with segmented legs," *International Journal of Robotics Research*, vol. 27, no. 8, pp. 919–934, 2008.

[21] A. Astolfi, G. Picardi, and M. Calisti, "Multilegged underwater running with articulated legs," *IEEE Transactions on Robotics*, 2021.

[22] S. Heim and A. Spröwitz, "Beyond basins of attraction: Quantifying robustness of natural dynamics," *IEEE Transactions on Robotics*, vol. 35, no. 4, pp. 939–952, 2019.

[23] H. Geyer, A. Seyfarth, and R. Blickhan, "Compliant leg behaviour explains basic dynamics of walking and running," *Proceedings of the Royal Society B: Biological Sciences*, vol. 273, no. 1603, pp. 2861–2867, 2006.

[24] R. J. Full and D. E. Koditschek, "Templates and anchors: neuromechanical hypotheses of legged locomotion on land." *The Journal of experimental biology*, vol. 202, no. Pt 23, pp. 3325–32, 1999. [Online]. Available: http://www.ncbi.nlm.nih.gov/pubmed/10562515

[25] M. H. Raibert, H. B. Brown Jr, and M. Chepponis, "Experiments in balance with a 3d one-legged hopping machine," *The International Journal of Robotics Research*, vol. 3, no. 2, pp. 75–92, 1984.

[26] A. Ruina, "The Simplest Walking Model : Stability , Complexity , and Scaling," vol. 120, no. April, pp. 281–288, 1998.

[27] A. Martin, V. Janssens, D. Caboor, J.-P. Clarys, and M. Marfell-Jones, "Relationships between visceral, trunk and whole-body adipose tissue weights by cadaver dissection," *Annals of human biology*, vol. 30, no. 6, pp. 668–677, 2003.

[28] M. Calisti and C. Laschi, "Morphological and control criteria for self-stable underwater hopping," *Bioinspiration & biomimetics*, vol. 13, no. 1, p. 016001, 2017.

[29] S. Gart, R. Alicea, W. Gao, J. Pusey, J. V. Nicholson, and J. E. Clark, "Legged locomotion in resistive terrains," *Bioinspiration & Biomimetics*, vol. 16, no. 2, p. 025001, 2021.

[30] M. Calisti, E. Falotico, and C. Laschi, "Hopping on uneven terrains with an underwater one-legged robot," *IEEE Robotics and Automation Letters*, vol. 1, no. 1, pp. 461–468, 2016.